High-resolution photoemission study of the discommensurate (5.55×5.55) Cu/Si(111) surface layer

H.-J. Neff, I. Matsuda, M. Hengsberger, F. Baumberger, T. Greber, and J. Osterwalder
Physik-Institut, Universität Zürich-Irchel, Winterthurerstrasse 190, CH-8057 Zürich, Switzerland
(Received 4 July 2001; revised manuscript received 29 August 2001; published 27 November 2001)

We have mapped the electronic bands of the ''quasi-(5×5)'' monolayer structure of Cu on Si(111) near the Fermi energy at high angular and energy resolution. Although this unusual system does not exhibit a true long-range periodicity, well-defined bands and sharp Fermi surface contours are observed. The fundamental Fermi surface inside the first surface Brillouin zone has the shape of a hexagon and possesses strong nesting features. However, no relation to the unusual translational symmetry could be established. Strong umklapp bands and Fermi surface contours are observed with umklapp vectors that correspond to the reciprocal lattice of the slightly expanded and rotated discommensurate Cu_2Si layer, and to that of the quasi-(5×5) domain pattern formed by the regular dislocation network. We find thus a one-to-one correspondence between the electronic bands and the complex structure model that has been established by Zegenhagen *et al.* [Phys. Status Solidi B **204**, 587 (1997)]. This suggests that the two-dimensional electron gas formed on this surface does not induce the formation of the discommensurate structure but rather takes a spectator role.

DOI: 10.1103/PhysRevB.64.235415 PACS number(s): 79.60.Dp, 73.20.−r, 73.22.−f, 73.30.+y

I. INTRODUCTION

The growth of copper on Si(111) has attracted not only academic but also technological attention for the past two decades and is nowadays one of the most relevant metal-on-semiconductor interfaces for modern device technology. One of the interesting issues in this system is the well-defined and stable interface layer formed during elevated-temperature growth. Examination of this layer by low-energy electron diffraction[1,2] (LEED) and He atom scattering[3] revealed a (5.55×5.55) periodicity that is not commensurate with the Si(111) substrate. These findings have stirred a lot of interest in the surface science community 10 years ago. Structural investigations came up with three different models for the local bonding, which involve three different surface stoichiometries. From Auger electron diffraction measurements, Chambers, Anderson, and Weaver[4] suggested a coplanar $CuSi_2$ structure where Cu atoms occupy the H_3 sites in a vertically compressed Si(111) surface double layer. Chambliss and Rhodin[5] have measured the position and the dispersion of the Cu $3d$ band by angle-resolved ultraviolet photoelectron spectroscopy (ARUPS). From comparing their data to band-structure calculations, they favor a simple CuSi structure with Cu substituting for Si in the S_u sites terminating the surface. A bit later, Zegenhagen *et al.*[6] were able to identify two inequivalent Cu sites by means of an x-ray standing wave study, thus completing the CuSi model by adding one additional Cu atom into H_3 sites to form a corrugated Cu_2Si layer. This model could recently be confirmed by Cu $2p$ x-ray photoelectron diffraction (XPD).[7]

While these probes were sensitive to the average local bonding geometry, they could not give further insight into the discommensurate[8] character of the layer. This aspect also proved to be a challenge to scanning tunneling microscopy (STM).[9–13] The pronounced bias dependence of the images[12] and the variety of local structures that invariably appear on STM topographs,[11] make determination of the surface unit cell and the film registry on the Si(111) substrate very difficult. The conclusions were that a dense network of misfit dislocations develops due to the large lattice mismatch,[9] that at least three electronically and structurally distinct local phases arrange to form a quasiperiodically ordered structure,[11] and that the observed quasi-(5×5) periodicity is the moiré periodicity arising from placing the Cu-Si layer on the (1×1) template of the Si(111) lattice plane.[12] In the latter work, it is conjectured that the layer is vertically compressed to be nearly planar, and that this compression is accompanied by a lateral expansion of 9.7% and a $\pm3.3°$ rotation, whereby a moiré period of $5.55a_{1\times1}$ results. Here, $a_{1\times1}=3.84$ Å is the Si(111) surface lattice vector. A complete tiling of the surface can be achieved by having three different types of domains that are connected via $5.55a_{1\times1}$. Earlier transmission electron microscopy (TEM) results have shown large domains of typically 1 μm size that show either a plus or a minus 3.5° rotation with respect to the substrate directions,[14] fully supporting this model. There is thus domain formation at two different length scales (ca. 20 Å, bounded by the dislocation network, and 1 μm for either clockwise or counterclockwise rotation). These results, comprehensively reviewed by Zegenhagen *et al.*[15] and schematically depicted in Fig. 1, for the convenience of the reader, gave a full flavor of the complexity of this interface, and the general interest has since decayed.[16]

More recently, metal-semiconductor interfaces have gained renewed interest from a different point of view. In the monolayer regime, some are found to represent low-dimensional materials that can exhibit exotic physical phenomena such as Peierls-like instabilities[18] and surface charge-density wave (CDW) formation.[19] For such scenarios the Fermi surface of the two-dimensional (2D) layer needs to have specific nesting features, i.e., parallel contours that can be connected by one particular so-called nesting vector $\vec{q}_c$, and that often render the electronic system quasi-one-dimensional.[20] The CDW transition is driven by a singularity in the electronic susceptibility occurring at the wave vector $\vec{q}_c$, which in the truly 1D electron gas is equal

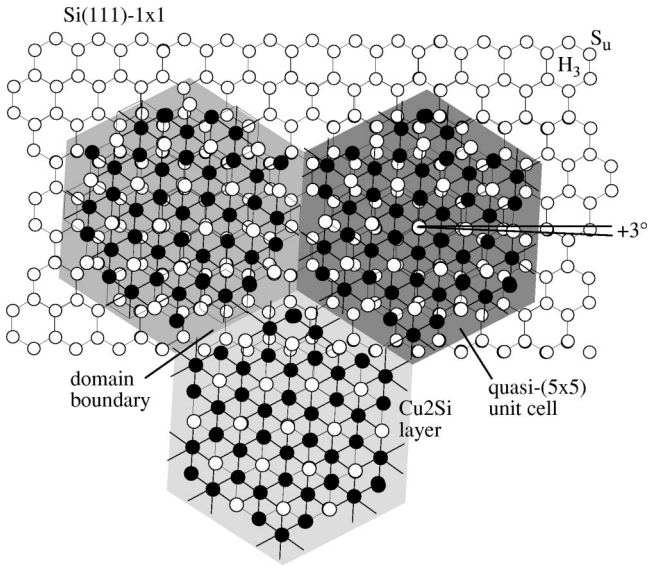

FIG. 1. Schematic representation of the structural model for the discommensurate quasi-5×5 Cu/Si(111) layer as described by Zegenhagen *et al.*[15] Silicon atoms are given as open circles, copper atoms as filled circles. The Cu_2Si layer replaces the outermost double layer of the unreconstructed Si(111)-1×1 surface, with Cu atoms occupying S_u and H_3 sites. This dense layer is laterally expanded by 9.7%, and the large lattice misfit leads to a regular dislocation network, bounding incommensurate domains (hexagons of variable gray). Within larger domains with size of up to micrometer, the layer structure is rotated by either plus or minus 3° away from the substrate orientation.

to $2k_F$ where k_F is the Fermi wave vector. The band filling thus defines the wave length of the CDW. Since, in real materials, the filling of such quasi-1D bands is largely determined by the detailed 2D (or even 3D) band structure, $\vec{q}_c$ can take on any arbitrary value and incommensurate CDW are, therefore, more the rule than the exception. Motivated by early photoemission Fermi surface data on the quasi-(5×5) Cu/Si(111) system,[21] which indicated that its Fermi surface is prone to nesting, *one may wonder if the discommensurate overlayer structure might not arise from a similar mechanism and thus be electronically driven.*

We have, therefore, engaged in a very careful high-resolution photoemission Fermi surface mapping experiment[22,23] on the quasi-(5×5) Cu/Si(111) interface in order to determine its detailed electronic structure near the Fermi level and to discuss it in the context of nesting scenarios that might be related to the (5.55×5.55) periodicity. The absence of true periodicity in the layer means that $k_\parallel$, the wave-vector component parallel to the surface, should not be a good quantum number. Therefore, the photoemission peaks measured at any given emission angle are due to a number of related states, and dispersion of bands with $k_\parallel$ should not be strictly applicable.[5] Nevertheless, we find photoemission features that are extremely sharp in $k_\parallel$ and rather sharp in energy. The shape of the Fermi surface is well apt for extended nesting, but the measured nesting vectors are in no conceivable relation to the quasi-(5×5) structure.

II. EXPERIMENTAL

The experiments were performed in a modified Vacuum Generators ESCALAB 220 spectrometer that is described elsewhere.[24] The Si(111)-7×7 surface was prepared by cycles of Ar^+ sputtering (500 V) at room temperature and consecutive flashing/annealing. The *n*-type crystal (0.07 Ω cm) of dimensions $1.0\times0.4\times0.03$ cm^3 was heated resistively. The quality and cleanliness of the surface were checked with LEED and x-ray photoelectron spectroscopy (XPS). From XPD measurements, we determined the crystal orientation to within better than 1°.

Copper was evaporated from a hot tungsten filament to give a deposition rate of about 0.1 monolayers (ML) per minute as calibrated by XPS measurements. The pressure was kept below 2×10^{-9} mbar during deposition. About 1–3 ML of Cu were deposited on the sample at room temperature. Subsequent heating of the crystal to temperatures of 500–600 °C reduced the Cu coverage to about 0.8 ML and led to the formation of the quasi-(5×5) phase as judged from the well-defined LEED pattern.

For the photoemission experiments He Iα (21.2 eV) and He IIα (40.8 eV) radiation was used for excitation, produced in a microwave-driven high-flux He discharge lamp with a toroidal grating monochromator (Gammadata Burklint AB, Sweden). The energy resolution of the electron analyzer was set to about 40 meV, the angular resolution to better than 1° full width at half maximum. Data acquisition was made either by taking series of energy spectra while scanning one photoelectron emission angle (polar angle θ or azimuthal angle ϕ) to produce energy dispersion plots, or by recording photoelectron intensities at the Fermi level while scanning both emission angles across the full hemisphere to produce Fermi surface maps.[24] The Fermi energy was determined by fitting the Fermi edge measured on an Ag polycrystal. All experiments were performed at room temperature, at a base pressure below 3×10^{-10} mbar. Typical measuring times for the individual data sets were about 5 h.

III. RESULTS AND DISCUSSION

In Fig. 2(a), the normal emission spectrum from a quasi-(5×5) Cu/Si(111) layer of 0.8 ML thickness is shown. It is dominated by the strong Cu 3*d* emission in the binding-energy region between 2 eV and 5 eV, in agreement with the earlier study by Chambliss and Rhodin.[5] An additional peak appears at 1.37 eV that they missed, maybe due to their limited energy (0.2 eV) and angular resolution, or due to different light polarization. We can identify the origin of this peak by comparing the spectrum to the normal emission spectrum from the clean Si(111)-7×7 surface that is given as the lower curve in Fig. 2(a), and which shows two prominent features at 2.0 eV and 0.9 eV, labeled as *B* and *S*2, respectively. The feature *B* is associated with a direct transition from the uppermost Si(111) bulk band of Λ_3 symmetry.[25] We have compared the dispersion of the 1.37 eV peak on the Cu/Si interface (see below) with the dispersion of feature *B* measured on the Si(111)-7×7 (not shown) and

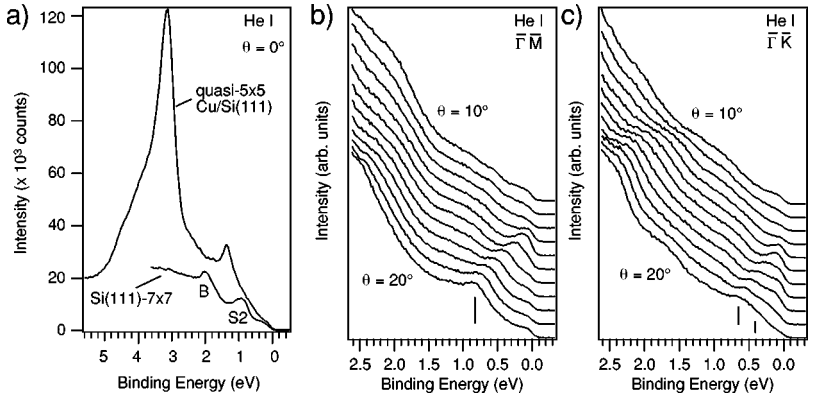

FIG. 2. (a) He I excited normal emission spectrum from the quasi-(5×5) Cu/Si(111) layer. For reference, a spectrum from clean Si(111)-7×7 is also shown with a bulk direct transition (B) and a surface state feature ($S2$) indicated. Note that the spectra are drawn to scale. (b) Angle-resolved photoemission spectra from the quasi-(5×5) Cu/Si(111) layer measured along the $\overline{\Gamma M}$ direction of the surface Brillouin zone for polar emission angles θ ranging from 10° to 20°, taken in 1° steps. One dispersing feature is indicated. (c) Same set of spectra measured along the $\overline{\Gamma K}$ direction. Two dispersing features are indicated.

found them to be very similar, which establishes the bulk origin of this extra spectral feature. Compared to the clean Si surface, the peak (B) appears here shifted by 0.63 eV to lower binding energy. This result indicates that band bending of the valence band towards the Fermi level has occurred on the surface. Since the binding energy of the valence band maximum (VBM) on the 7×7 surface is ≈0.63 eV,[26] the VBM for the quasi-(5×5) surface is estimated to be located very close to the Fermi level. This indicates that a p-type inversion layer is created by the formation of the interface.[27]

In the remainder of this paper, we want to focus on the electronic bands in the vicinity of the Fermi energy ϵ_F. Figures 2(b,c) show series of ARUPS spectra taken with a photon energy of 21.22 eV (He Iα radiation) along the $\overline{\Gamma M}$ and $\overline{\Gamma K}$ directions of the Si(111) (1×1) surface Brillouin zone (SBZ). All the spectra show a Fermi edge and a steep background beginning immediately below ϵ_F and rising monotonously towards the onset of the Cu $3d$ band. Superimposed on this background is a fast-dispersing feature that can be seen along both directions at binding energies below 1 eV. The particular polar angle range from $\theta=10°$ to $\theta=20°$ has been selected in order to illustrate the Fermi level crossings of this feature. It is obvious that the quasi-(5×5) surface is metallic. In the previous ARUPS measurements on this surface by Chambliss and Rhodin,[5] they also have observed the same electronic states near the Fermi level. However, in their spectra these features are much broader than those of the present study due to their poorer energy resolution, and they could not conclude whether the observed surface state crosses the Fermi level or not. The metallicity that we find is consistent with the data of an early inverse photoemission study of this interface[28] where a structure of relatively high intensity was observed at the Fermi level. From our very detailed measurements of the metallic states it emerges that there are actually two features that disperse along $\overline{\Gamma K}$ and that cross the Fermi level at a few degrees apart (see below).

In order to trace all the Fermi-level crossings as a function of $k_\parallel$, we have compiled the photoemission intensities at ϵ_F for all emission angles and plotted them in the $k_\parallel$ plane.[29] At a given azimuth, $k_\parallel$ is calculated as $k_\parallel=1/\hbar\sqrt{2m(h\nu-\Phi)}\sin\theta$ where θ is the polar emission angle measured from the surface normal, $h\nu$ the photon energy, m the free-electron mass and Φ the work function that is taken to be 5.3 eV.[5] Figure 3(a) shows the resulting Fermi surface contours obtained with He Iα excitation. Centered inside the first Si(111) (1×1) SBZ a regular hexagon appears with its sides parallel to the zone boundaries. Stronger replica of these straight hexagon sides appear in all six neighboring SBZ's, showing a strictly sixfold rotational symmetry. The *intensities* of the contours, on the other hand, are modulated to give only a threefold symmetry. The photoemission matrix elements responsible for the measured intensities are thus sensitive to the threefold symmetry of the local bonding configuration within the Cu_2Si film.[7]

The observed Fermi-level crossings are extremely sharp in k space. This is clearly seen in momentum distribution curves (MDC's), i.e., in intensity line scans across the Fermi surface map. The maxima near 0.5 and 1.5 $Å^{-1}$ in Fig. 3(b) are very sharp and reproduce well in the two inequivalent $\overline{\Gamma M}$ directions. The curves have been sampled with 1° steps in polar angle, meaning that the dominant peak in the second SBZ has a full width at half maximum of less than 3°. The precise Fermi wave vector $\vec{k}_F^{(1)}$ measured from $\overline{\Gamma}$ is found to be 0.48(2) $Å^{-1}$, which equals 0.51(2) times the distance $\overline{\Gamma M}=0.945$ $Å^{-1}$ on the Si(111) (1×1) surface. The two curves along the $\overline{\Gamma M}$ and $\overline{\Gamma M'}$ directions illustrate the marked inequivalence with respect to photoemission intensities. In Fig. 3(c), we show the $k_\parallel$ dispersion of the contours in the 2nd SBZ along the dashed curve (A-B) indicated in Fig. 3(a). Four pairs of metallic states are clearly identified that are separated in azimuth angle by 6.5° within each pair. Since this azimuthal scan samples the second SBZ's not far from equivalents of the $\overline{\Gamma M}$ line, and since there is only one strong Fermi-level crossing along the $\overline{\Gamma M}$ direction, these data indicate that the photoemission measurement picks up Fermi surface contours simultaneously from the two micrometer-sized domains that exhibit either a clockwise or

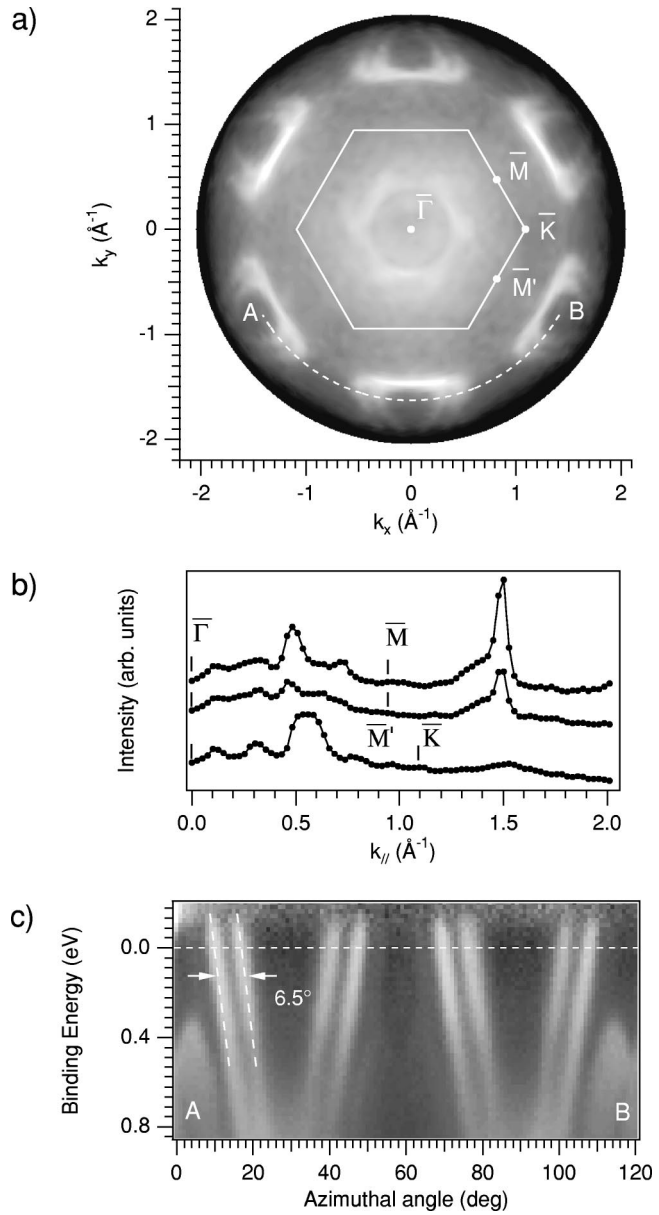

FIG. 3. (a) He I ($h\nu=21.22$ eV) excited photoemission Fermi surface map from a quasi-(5×5) Cu/Si(111) layer. The photoemission intensity at the Fermi level is mapped as a function of the emission angles and then plotted in parallel projection, i.e., as a function of $k_\parallel$, in a linear gray scale. The Si(111)-(1×1) surface Brillouin zone is indicated together with high-symmetry points. The data have been threefold averaged in order to improve the statistical accuracy of the data. (b) Line scans of the He I photoemission intensity at ϵ_F as a function of $k_\parallel$ for the quasi-(5×5) Cu/Si(111) interface along the $\overline{\Gamma M}$ direction ($[11\bar{2}]$ azimuth of the threefold Si(111) surface) (top), the $\overline{\Gamma M'}$ direction (middle) and along the $\overline{\Gamma K}$ line (bottom). (c) Photoemission dispersion plot for the quasi-(5×5) Cu/Si(111) interface for a polar angle $\theta=52°$ and an azimuth angle section of 120° along the line AB indicated in (a). The data are representing the photoemission intensities in a linear gray scale and have been normalized to constant integrated intensity along each horizontal line, i.e., at each binding energy. By this procedure the intensity drop at ϵ_F is lifted and the band dispersion can be traced slightly further. The angular separation of two bands due to the presence of rotational domains is indicated.

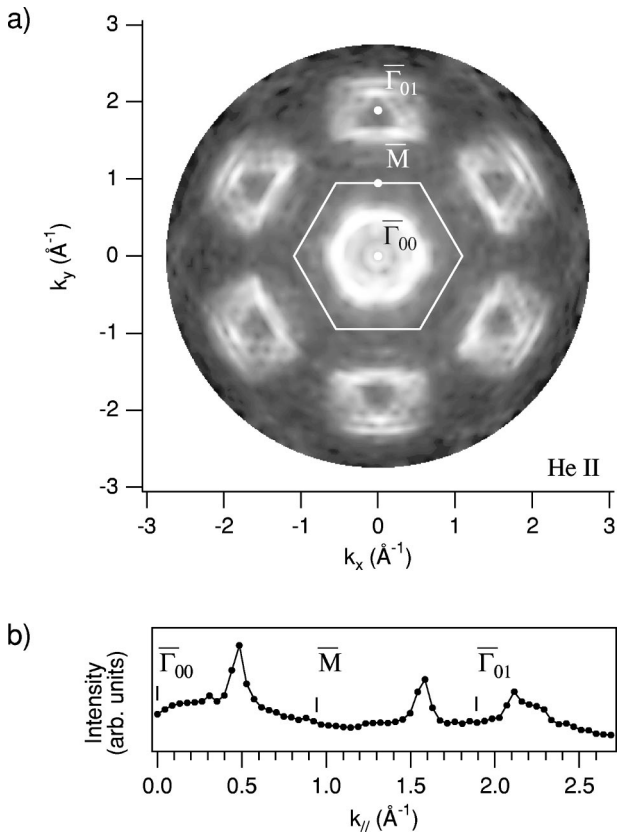

FIG. 4. (a) He II ($h\nu=40.8$ eV) excited photoemission Fermi-surface map from a quasi-(5×5) Cu/Si(111) layer. The first Si(111)-(1×1) surface Brillouin zone and the reciprocal lattice vectors $\bar{\Gamma}_{00}$ and $\bar{\Gamma}_{01}$ are indicated. (b) Line scan of the He II photoemission intensity at ϵ_F as a function of $k_\parallel$ along the $\overline{\Gamma M}$ direction.

counterclockwise rotation of about 3° with respect to the substrate low-index directions.[14]

From such data we may now venture to measure the exact size and shape of the Fermi surface. In order to confirm the visual impression of a hexagonal shape, we inspect the line scan along the $\overline{\Gamma K}$ direction, which is also shown in Fig. 3(b). For a regular hexagon with the measured value for $\vec{k}_F^{(1)}$ of 0.48(2) Å^{-1} along the $\overline{\Gamma M}$ direction, we expect a corner distance of $\vec{k}_F^{(2)}=\vec{k}_F^{(1)}\times2/\sqrt{3}$, which is 0.55(2) Å^{-1}. Although the width of the peak in Fig. 3(b) indicates the presence of two bands crossing the Fermi level, the one further out in $k_\parallel$ is very nearly at this position. The conclusion from this preliminary analysis is thus that the quasi-(5×5) Cu/Si(111) layer has to first order a Fermi surface with the shape of a hexagon that spans very nearly half the linear dimensions of the (1×1) SBZ. However, complications arise due to the two rotational domains and due to additional features [see, e.g., Fig. 3(b)] related with the quasi-(5×5) superstructure, as will be discussed further below.

In order to verify the 2D nature of the interface-related bands, we have measured a corresponding data set by using He IIα radiation ($h\nu=40.8$ eV). The Fermi surface map for this photon energy is shown in Fig. 4(a), again with the (1×1) SBZ indicated in order to give the relevant k space

scale. At the first glance, the observed contours give a quite similar picture as the ones in the He Iα data. The hexagonal shape of the Fermi surface in the first SBZ is not so evident here, which is mainly due to the limited sampling density in these 2D images as defined by 2° steps in polar angle. We have used the same angular sampling density as for the He Iα data, which translates into a lower point density in $k_\parallel$ for the higher photon energy of He IIα radiation. Conversely, one reaches further out into the neighboring (1×1) SBZ's, thus covering the entire Fermi surface at six more places. Where we have overlap with the He I data, the contours look quite similar, with a rather straight section parallel to the zone boundaries and the split contours that appear to bend around the zone centers [e.g., $\bar{\Gamma}_{01}$ in Fig. 4(a)]. However, the contours in the outer zones show a lot more details that no longer convey the simple picture of a hexagonal Fermi surface centered in the zone. Moreover, taking more precise measurements from the MDC along the $\overline{\Gamma M}$ direction [Fig. 4(b)], we realize that the Fermi surface in the first SBZ is still well centered between $\bar{\Gamma}$ and $\bar{M}$, like in the He I data, but the same is no longer true in the second SBZ, where there is a marked shift of the main contour to higher values of $k_\parallel$. Rather than completing the picture, this additional data set at higher photon energy raises more questions.

We suggest that the answer to this puzzling and energy-dependent deviation from periodicity in k space lies in the quasiperiodic structure of the Cu/Si overlayer leading to umklapp scattering with discommensurate surface lattice vectors. Such umklapp processes can lead to strong additional photoemission features as a function of angle and energy.[30–32] In order to visualize umklapp bands, Fig. 5 displays photoemission dispersion plots along the $\overline{\Gamma M}$ and $\overline{\Gamma K}$ directions. The white dashed lines represent the band edges of the bulk bands projected onto the Si(111) (1×1) SBZ.[26] The metallic states are positioned well within the bulk band gap, and the states are thus clearly identified as surface states. The two strong Fermi surface crossings near 0.5 and 1.5 Å^{-1} along the $\overline{\Gamma M}$ direction, which were discussed above [Fig. 3(b)], are associated with two dominant bands [Fig. 5(a)] that are, at first sight, related to each other by the symmetry of the Si(111)-(1×1) Brillouin zone (see below). A similar but broader band appears along the $\overline{\Gamma K}$ direction [Fig. 5(b)]. These data clearly identify the hexagonal Fermi surface centered at $\bar{\Gamma}$ to be of the hole type. In addition to these dominant bands, there are a number of weaker bands that also cross the Fermi level. These crossings, some of which are marked by white lines, can also be seen as extra peaks in the MDC's of Fig. 3(b), clearly visible on either side of the main Fermi surface peak in the first SBZ. Along the $\overline{\Gamma M}$ line, these features appear to be roughly periodic, with umklapp vectors of the order of 1/11 of a Si(111)-(1×1) reciprocal lattice vector $q_{1\times1}$ [indicated by arrows in Fig. 5(a)]. This value corresponds to half the periodicity $q_{5\times5} = 1/5.55\ q_{1\times1}$ of the quasi-(5×5) lattice. In order to understand this reduced spatial frequency, we have to consider the 2D character of the k-space geometry. The situation is sketched in Fig. 6(a). Due to the sixfold arrangement of quasi-(5×5) umklapp vectors, and due to the hexagon shape

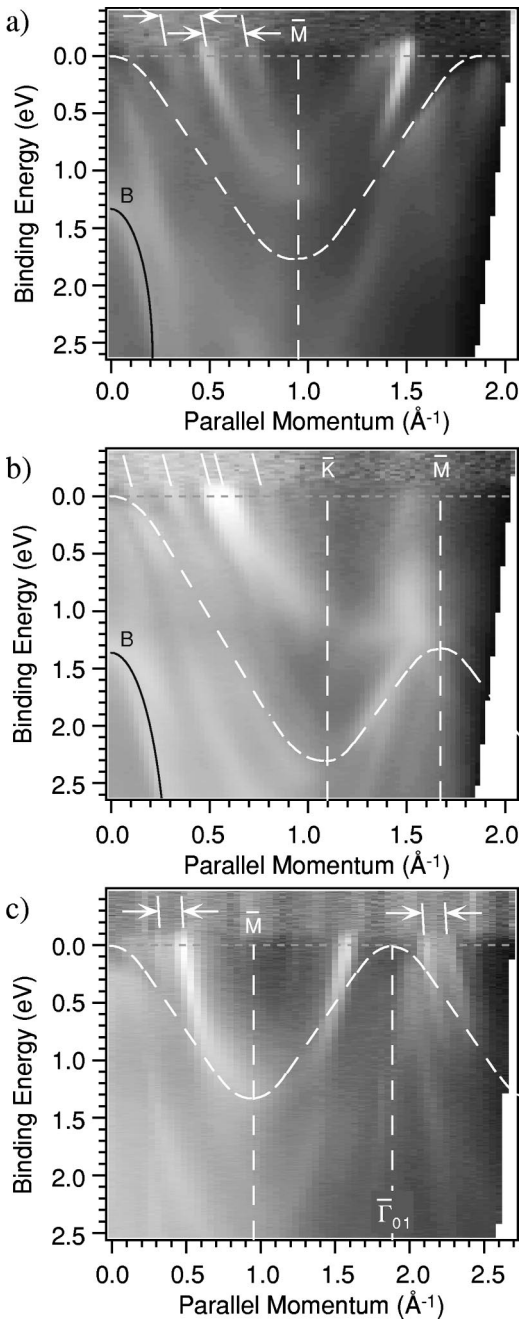

FIG. 5. Photoemission dispersion plots for the quasi-(5×5) Cu/Si(111) interface. The data sets have been compiled from polar scans of photoemission spectra by mapping the polar angle onto $k_\parallel$ and by representing the photoemission intensities in a linear gray scale. White dashed lines indicate the edge of bulk bands projected into the (1×1) surface Brillouin zone. White lines, some of which are spaced by 1/11 of a (1×1) reciprocal lattice vector (white arrows), indicate Fermi level crossings of some fundamental bands and some umklapp bands. (a) He I excited spectra measured along the $\overline{\Gamma M}$ direction. (b) He I excited spectra measured along the $\overline{\Gamma K}$ direction. The same normalization as in Fig. 3(c) has been applied. (c) He II excited spectra measured along $\overline{\Gamma M}$.

of the Fermi surface, the contours from two umklapp vectors that lie 120° apart combine to form extra straight lines constituted by two parallel hexagon sides. These extra lines are

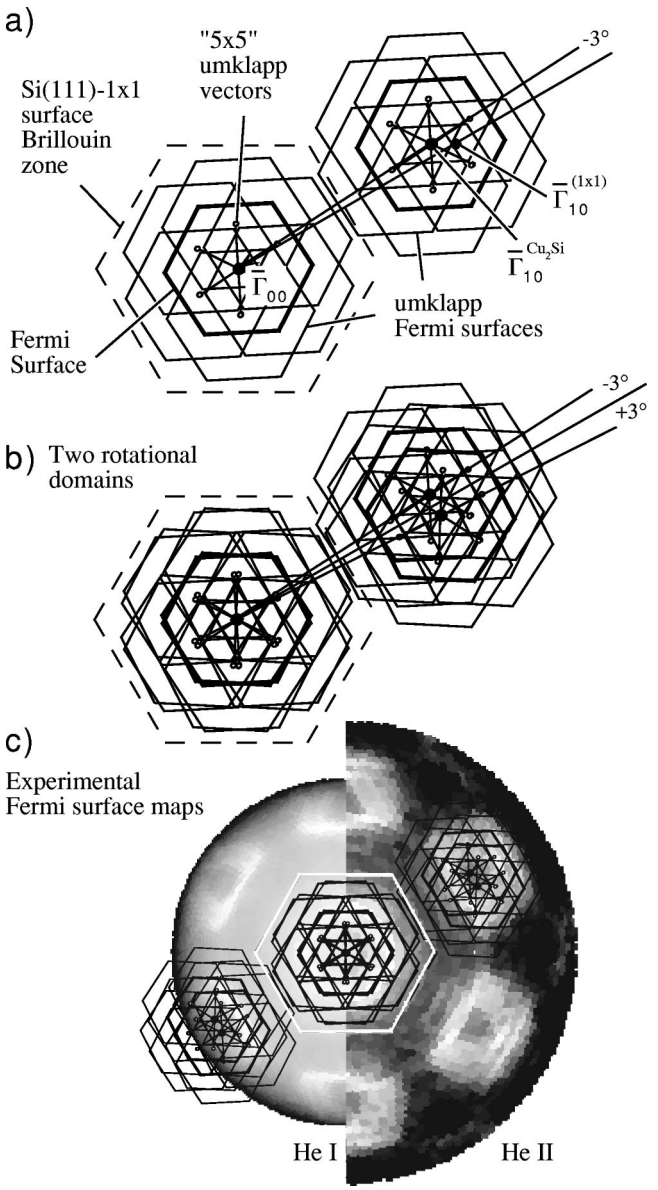

FIG. 6. (a) Schematic drawing of the various Fermi surface contours obtained in the first and second surface Brillouin zone by quasi-(5×5) umklapp scattering of the hexagonal Fermi surface. In the second SBZ, the umklapp vectors $\vec{q}_{(5\times5)}$ are centered at the reciprocal lattice point $\overline{\Gamma}_{10}^{Cu_2Si}$ of the slightly expanded and rotated Cu_2Si layer and not at $\overline{\Gamma}_{10}^{(1\times1)}$ of the underlying Si(111)-(1×1) lattice. (b) Complex umklapp pattern of Fermi surface contours obtained by superimposing two domains rotated by $\pm3°$. (c) Overlay of this umklapp pattern of Fermi surface contours on the real data. The He I and He II excited Fermi surfaces have been brought to matching *k*-vector scales.

situated just halfway between the Fermi surface centered at $\overline{\Gamma}$ and the contour of the first umklapp vector along the $\overline{\Gamma M}$ line. They are thus responsible for the apparent reduction of spatial frequency along this direction. The Fermi surface near the hexagon corners ($\overline{\Gamma K}$ direction) is sampled in these halfway features rather than that along the $\overline{\Gamma M}$ direction. This explains why the Fermi-level crossings marked in Fig. 5(a) are not precisely separated by 1/2 $q_{5\times5}$. In fact, these data imply a slight deviation from a perfectly hexagonal shape of the Fermi surface, with the hexagon corners pushed slightly outwards. This impression may well arise due to the presence of two bands crossing the Fermi level at very close positions along the $\overline{\Gamma K}$ direction [see Fig. 3(b)].

The dispersion plot for the electronic bands along the $\overline{\Gamma K}$ direction, which is shown in Fig. 5(b), shows the two-band character of the main feature much more clearly. The broad peak at the Fermi level separates into two distinct bands at binding energies higher than 0.5 eV. Along this direction, the 2D umklapp vectors lead to features with a periodicity of $1/\sqrt{3}\times q_{5\times5}$ according to the model of Fig. 6(a). In this *k*-space section, we realize the high degree of complexity that arises due to this strong umklapp scattering also at higher binding energies. A one-to-one identification of individual bands is not possible here without the help of a band-structure calculation for the Cu/Si interface. Fortunately, the situation at the Fermi level appears to be simpler due to the presence of one dominating band or maybe two bands that are nearly degenerate except along the $\overline{\Gamma K}$ direction.

We now address the problem of the inconsistent positions of Fermi surface contours in the second SBZ, as observed with He I and He II excitation [cf. Figs. 3(b) and 4(b)]. In doing so, we need to consider all the subtleties of the structural model as described by Zegenhagen *et al.*,[15] i.e., that the nearly coplanar Cu_2Si layer is laterally expanded by 9.7% and rotated by $\pm3°$ relative to the underlying Si(111) lattice within the individual domains formed by the quasi-(5×5) dislocation network. Clarifying the origin of the surface state requires a band structure calculation for this surface compound, which is not available to the present study. Nevertheless we can speculate on the character of the electronic states that cross the Fermi energy. In this energy region one expects Cu $4s$, Cu $3d$ and Si $3sp$ valence electrons. Previous ARUPS and x-ray absorption studies[33,34] have shown that the hybridization of Cu $3d$ with Si valence states lies in-plane of the quasi-(5×5) layer and that of Cu $4s$ lies perpendicular to the layer. This indicates that the Cu-Si bonding in the quasi-(5×5) layer is likely to follow the typical transition-metal-silicide bonding scheme, e.g., in a bulk Cu silicide (Cu_3Si),[35] but in two dimensions. Thus, one would expect that the metallic state that is observed in the present study, is a partially filled antibonding state resulting from an in-plane hybridization of Cu $3d$ and Si $3sp$ states. The measured band dispersion and the holelike character of the Fermi surface are fully consistent with this antibonding picture.

An important consequence of this assignment is that these states are weakly coupled to the underlying substrate,[33] and that the electrons thus probe essentially the potential of the expanded and slightly rotated lattice within the Cu_2Si layer. The relevant periodicity is thus not described by the Si(111)-(1×1) reciprocal lattice but rather by one that is shrunk by roughly 10% and rotated by $\pm3°$. Figure 6(a) illustrates the resulting geometries that arise from surface umklapp scattering off these periodicities. The Fermi surface related with the antibonding band is sketched as a bold hexagon centered at the origin $\overline{\Gamma}_{00}$ of the two-dimensional momentum space. A

replica of this Fermi surface is plotted, again in bold lines, in one of the neighboring SBZ's. Note that this contour is not centered around the reciprocal lattice point $\overline{\Gamma}_{10}$ of the Si(111)-(1×1) surface, but around the slightly shifted $\overline{\Gamma}_{10}^{Cu_2Si}$ point associated with the expanded and rotated Cu_2Si layer. Within each rotational domain, the periodic network of dislocations leads to the (5.55×5.55) or quasi-(5×5) periodicity relative to the Si(111)-(1×1) lattice. Umklapp scattering off the dislocation network potential thus produces Fermi surface replica centered at positions $\overline{\Gamma}_{00}+\vec{q}_{(5\times5)}$ and $\overline{\Gamma}_{10}^{Cu_2Si}+\vec{q}_{(5\times5)}$, where $\vec{q}_{(5\times5)}$ is one of the six symmetry-equivalent quasi-(5×5) reciprocal lattice vectors. Figure 6(a) shows the intricate line pattern that is formed by the entity of all these umklapp Fermi surfaces, with the apparent reduction of spatial frequencies along the $\overline{\Gamma M}$ direction discussed earlier. The presence of roughly equal amounts of domains rotated by $+3°$ or $-3°$ should lead to the rather messy picture plotted in Fig. 6(b). In Fig. 6(c), the complete umklapp pattern is overlayed upon the experimental He I and He II Fermi surface maps, all of which are given in the same momentum scale. The direct comparison yields some interesting observations:

(i) The experimental data show some but not all of the umklapp Fermi surface contours.

(ii) Where they are observed, they appear at positions that are predicted by our simple model.

(iii) The measured intensities of the contours vary strongly within the individual SBZ and from one to the other.

(iv) The relative intensities of different umklapp contours are very different for He I and He II excitation.

(v) The dominant contours measured in the second SBZ correspond to quasi-(5×5) umklapp bands, and not to the Fermi surface centered around $\overline{\Gamma}_{10}^{Cu_2Si}$. Different umklapp vectors $\vec{q}_{(5\times5)}$ dominate for He I and for He II.

Overall, this comparison gives convincing evidence that the momentum distribution of the measured surface state reflects all aspects of the complete structural model as described by Zegenhagen *et al.*[15]

The striking dependence of the umklapp scattering intensities on the excitation energy can be understood on the basis of the one-step model of photoemission.[36] The final state is here taken to be a time-reversed LEED state. During the characterization of the quasi-(5×5) phase by LEED, we noticed a pronounced change of relative intensities within the quasi-(5×5) spot sets as a function of electron energy. This is shown in Fig. 7, where LEED patterns at three different energies are given. At 100 eV the quasi-5×5 spots around each fundamental spot have very similar weights, while at the lower energies, the spots closer to the (0,0) beam are significantly stronger. At 44 eV and 100 eV there is also an increasing threefold component in the spot-intensity distribution due to the growing contribution of substrate scattering. Although we have not studied these effects systematically, the LEED patterns indicate that the energy dependence of the umklapp scattering intensities is a final-state effect. It is

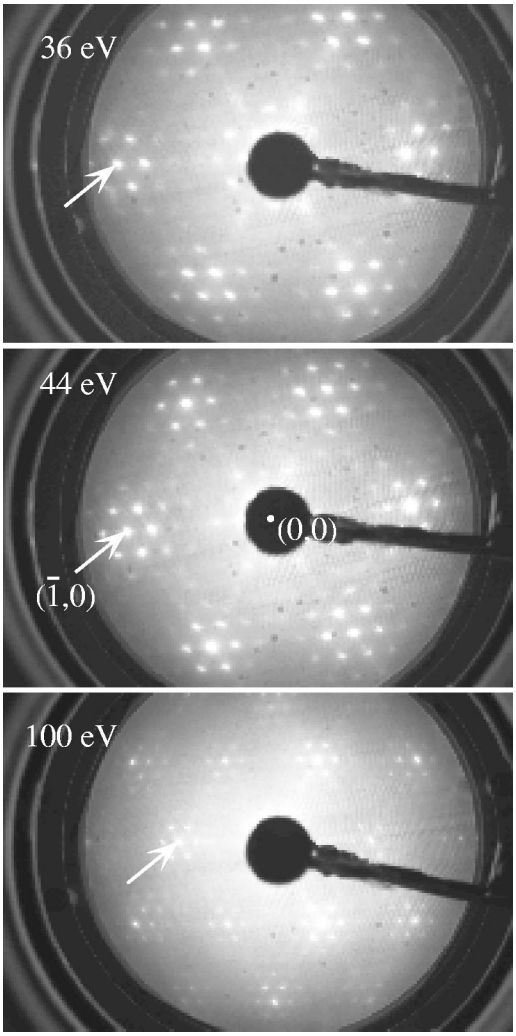

FIG. 7. LEED patterns from the quasi-5×5 Cu/Si(111) interface, taken at near-normal beam incidence and at three different electron energies: 36 eV, 44 eV, and 100 eV. The arrows indicate the positions of one of the six first-order Si(111) substrate spots.

worth noting that our LEED patterns do not show the $\pm3°$ rotation of spots expected from the presence of rotational domains. At the energies that we used, which lie between 36 eV and 100 eV, electron diffraction from the underlying Si(111) substrate appears to be strong enough to lock the quasi-(5×5) spots at positions that are centered around the (1×1) reciprocal lattice vectors. There are reports that LEED patterns taken at very low energies show the presence of the rotated domains by a $\pm3°$ azimuthal splitting of the quasi-(5×5) spots centered around the (0,0) spot.[37] The diffraction intensities must be coming from the first monolayer alone, like in our photoemission study of the metallic band.

The strong momentum dependence of the umklapp intensities is more interesting and surprising. In the following, we discuss two mechanisms that are known to distribute intensities nonuniformly over momentum space.

Coherent photoemission from inequivalent atoms within the Cu_2Si surface unit cell can interfere to modulate the measured intensity in momentum space. This is conveniently described by the so-called photoemission structure factor,[38,39]

which can distribute band intensities in a characteristic fashion from zone to zone,[38] but also within each SBZ.[39] We have performed a calculation of the photoemission structure factor by using a simple tight-binding model[40] for the Cu_2Si layer with spherically symmetric Cu $3d$ and Si $3p$ orbitals placed on the atomic sites. Preliminary results predict strong photoemission of the fundamental band (umklapp scattering is not contained in this model) inside the first SBZ and weak emission in all six neighboring zones, with little variation inside each zone except for enhanced emission along the zone boundaries. Although the calculation may be oversimplified, these results might rationalize why the fundamental band is suppressed relative to the umklapp bands in the second SBZ's, as is observed in Figs. 3–6. However, a more sophisticated calculation including the detailed electronic structure and surface umklapp scattering is required in order to fully clarify this effect.

A different mechanism that can redistribute photoemission intensities in momentum space has recently been discussed by Voit *et al.*[41] They calculate the single-particle spectral function for solids with competing periodic potentials. The solutions to their simple model show two things: main bands and bands folded by the periodic potentials repell each other wherever they are close in energy and momentum and form energy gaps where they cross. Moreover, there is a shift of spectral weight from main bands to folded bands near these crossing points. This is due to the coherent interaction of the quasiparticles with the periodic potentials, and as such this is an initial-state effect and not to be confused with umklapp scattering in the final state, although the momentum shifts of the folded bands are the same. The quasi-(5×5) Cu/Si(111) surface is obviously a system with strongly competing potentials, and the Voit model should thus be relevant.

A complete analysis of the observed umklapp band intensities needs to combine all these discussed initial-state and final-state processes and is thus a formidable task and beyond the scope of this paper. Preliminary results show that applying the Voit model to a single tight-binding antibonding band, parametrized to match the fundamental Fermi surface in the first SBZ, can reproduce almost quantitatively the many bands shown in the dispersion plots of Fig. 5 as far as band positions are concerned (not shown). Some significant spectral weight shift to folded bands occurs in the second SBZ, qualitatively in accordance with the experimental data, but for a correct description of umklapp band intensities, umklapp scattering in the final state needs to be considered as well (see above). The periodicity of the underlying Si(111) substrate was found to play no significant role.

Let us now discuss possible scenarios for the formation of the quasi-(5×5) structure of the Cu_2Si layer. As described in the introduction, a metallic system in reduced dimensions becomes unstable against a lattice distortion due to the interaction of the electrons near the Fermi level with phonons at $2k_F$. The strength of this interaction scales with the degree of Fermi surface nesting, and if it is strong enough, it manifests itself as a periodic lattice distortion and the formation of a charge-density wave. The hexagon-shaped Fermi surface of the quasi-(5×5) Cu/Si(111) surface does show some nesting, and we can identify a nesting vector of $2k_F = 0.96(2)$ Å^{-1} oriented $\pm3°$ away from the $\overline{\Gamma M}$ direction. However, this value is in no simple relationship to any of the periodicities present on this surface: $\overline{\Gamma}_{10}$ of the Si(111)-(1×1) is at 1.89 Å^{-1}, $\overline{\Gamma}_{10}^{Cu_2Si}$ at 1.72 Å^{-1}, and $q_{(5\times5)}$ is 0.34 Å^{-1}. The closest match would be achieved with a (2×2) reconstruction with respect to the underlying Si(111) lattice, but there is no indication for such a reconstruction within the film, at least not at room temperature. Moreover, the data of Fig. 5 show clear Fermi-level crossings for all observed bands with no gap formation at E_F. We may, therefore, reasonably conclude that the formation of the quasi-(5×5) structure is due to the near balance between the adsorbate-substrate interaction and the local bonding within the Cu_2Si layer,[15] and that none of the more exotic scenarios apply.

IV. CONCLUSIONS

We have performed Fermi surface and band mapping measurements by high-resolution photoemission spectroscopy to study the electronic structure of the quasi-(5×5) Cu/Si(111) surface near the Fermi level. It is clearly established that the surface is metallic. The Fermi surface is of the hole type; it has a hexagonal shape and spans half the linear dimensions of the Si(111)-(1×1) SBZ. In addition, several umklapp bands and Fermi surface contours are observed that relate directly to the complete structural model of the system:[15] since the metallic band is associated with electrons that hybridize strongly within the Cu_2Si layer and weakly perpendicular to the film, the basic periodicity is that of the expanded film and not that of the underlying substrate. In the second SBZ's the bands from the two rotational domains are well resolved, and quasi-(5×5) umklapp bands dominate over the fundamental bands, with a strong dependence of spectral weight on momentum and on excitation energy. Although some nesting appears to be present due to the hexagonal shape of the Fermi surface, there seems to be no conceivable connection to the formation of the quasi-(5×5) structure. The present study demonstrates that high-resolution Fermi surface and band mapping experiments with photoemission spectroscopy is a very powerful tool to study such complex systems as the discommensurate quasi-(5×5) Cu/Si(111) surface.

ACKNOWLEDGMENTS

We thank W. Deichmann for his assistance with these experiments, and M. De Santis and G. Rossi for bringing this system to our attention. This work was supported by the Swiss National Science Foundation.

[1] E. Daugy, P. Mathiez, F. Salvan, and J.M. Layet, Surf. Sci. **154**, 267 (1985).
[2] H. Kemmann, F. Müller, and H. Neddermeyer, Surf. Sci. **192**, 11 (1987).
[3] R.B. Doak and D.B. Nguyen, Phys. Rev. B **40**, 1495 (1989).
[4] S.A. Chambers, S.B. Anderson, and J.H. Weaver, Phys. Rev. B **32**, 581 (1985).
[5] D.D. Chambliss and T.N. Rhodin, Phys. Rev. B **42**, 1674 (1990).
[6] J. Zegenhagen, E. Fontes, F. Grey, and J.R. Patel, Phys. Rev. B **46**, 1860 (1992).
[7] M. De Santis, M. Muntwiler, J. Osterwalder, G. Rossi, F. Sirotti, A. Stuck, and L. Schlapbach, Surf. Sci. **477**, 179 (2001).
[8] The ordering of an adlayer on a substrate is dictated by two competing forces, the adsorbate-adsorbate interaction and the adsorbate-substrate interaction. If the adsorbate-adsorbate interaction is dominant, the adsorbate layer may be incommensurate. If the adsorbate-substrate interaction is dominant, the adlayer is usually commensurate. If the two forces are competitive, the resulting structure can be discommensurate: weakly incommensurate domains form in which the adsorbate layer is highly strained. These domains are separated by a regular network of dislocations, where the strain is released (see, e.g., Ref. 15).
[9] R.J. Wilson, S. Chiang, and F. Salvan, Phys. Rev. B **38**, 12 696 (1988).
[10] S. Tosch and H. Neddermeyer, Surf. Sci. **211/212**, 133 (1989).
[11] J.E. Demuth, U.K. Koehler, R.J. Hamers, and P. Kaplan, Phys. Rev. Lett. **62**, 641 (1989).
[12] K. Mortensen, Phys. Rev. Lett. **66**, 461 (1991).
[13] R.A. Simão, C.A. Achete, and H. Niehus, J. Vac. Sci. Technol. A **15**, 1531 (1997).
[14] K. Takayanagi, Y. Tanishiro, T. Ishitsuka, and K. Akiyama, Appl. Surf. Sci. **41/42**, 337 (1989).
[15] J. Zegenhagen, P.F. Lyman, M. Böhringer, and M.J. Bedzyk, Phys. Status Solidi B **204**, 587 (1997).
[16] In a very recent paper (Ref. 17) the structure inside the quasi-5 $\times 5$ unit cells has been refined in a model that is, in some respects, at variance with the Zegenhagen model (Ref. 15). However, as far as the periodicities are concerned that are relevant for the observations in this paper, the Zegenhagen model holds and we restrict our discussion to this model.
[17] T. Kawasaki, T. An, H. Ito, and T. Ichinokawa, Surf. Sci. **487**, 39 (2001).
[18] H.W. Yeom, S. Takeda, E. Rotenberg, I. Matsuda, K. Horikoshi, J. Schäfer, C.M. Lee, S.D. Kevan, T. Ohta, T. Nagao, and S. Hasegawa, Phys. Rev. Lett. **82**, 4898 (1999).
[19] J.M. Carpinelli, H. Weiteung, E.W. Plummer, and R. Stumpf, Nature (London) **381**, 398 (1996).
[20] G. Grüner, *Density Waves in Solids* (Addison-Wesley, Reading, MA, 1994).
[21] M. De Santis, A. Stuck, J. Osterwalder, F. Sirotti, and G. Rossi, Vuoto **21**, 200 (1991).
[22] P. Aebi, J. Osterwalder, R. Fasel, D. Naumovic, and L. Schlapbach, Surf. Sci. **307-309**, 917 (1994).
[23] J. Osterwalder, Surf. Rev. Lett. **4**, 391 (1997).
[24] T. Greber, O. Raetzo, T.J. Kreutz, P. Schwaller, W. Deichmann, E. Wetli, and J. Osterwalder, Rev. Sci. Instrum. **68**, 4549 (1997).
[25] R.I.G. Uhrberg, G.V. Hansson, J.M. Nicholls, P.E.S. Persson, and S.A. Flodström, Phys. Rev. B **31**, 3805 (1985).
[26] R.I.G. Uhrberg and B.V. Hansson, Crit. Rev. Solid State Mater. Sci. **17**, 133 (1991).
[27] H. Lüth, *Surfaces and Interfaces of Solids* (Springer-Verlag, Berlin, 1993), p. 318.
[28] J.M. Nicholls, R. Salvan, and B. Reihl, Phys. Rev. B **34**, 2945 (1986).
[29] The data have been analyzed by the XPDPLOT package written by R. Fasel and R. A. Agostino, University of Fribourg.
[30] J.F. van der Veen, F.J. Himpsel, and D.E. Eastman, Solid State Commun. **34**, 33 (1980).
[31] J. Osterwalder, P. Aebi, P. Schwaller, L. Schlapbach, M. Shimoda, T. Mochiku, and K. Kadowaki, Appl. Phys. A: Solids Surf. **60**, 247 (1995).
[32] M. Hengsberger, D. Purdie, M. Garnier, K. Breuer, and Y. Baer, Surf. Sci. **405**, L491 (1998).
[33] M. Sancrotti, Maurizio Sacchi, Oumar Sakho, and Giorgio Rossi, Phys. Rev. B **44**, 1958 (1991).
[34] G. Rossi, Surf. Sci. Rep. **7**, 1 (1987).
[35] G. Rossi and I. Lindau, Phys. Rev. B **28**, 3597 (1983).
[36] P.J. Feibelman and D.E. Eastman, Phys. Rev. B **10**, 4932 (1974).
[37] T. Yasue, T. Koshikawa, M. Jalochowski, and E. Bauer, Surf. Sci. **480**, 118 (2001).
[38] E.L. Shirley, L.J. Terminello, A. Santoni, and F.J. Himpsel, Phys. Rev. B **51**, 13 614 (1995).
[39] H. Daimon, S. Imada, H. Nishimoto, and S. Suga, J. Electron Spectrosc. Relat. Phenom. **76**, 487 (1995).
[40] W. A. Harrison, *Electronic Structure and the Properties of Solids* (W. H. Freeman and Company, San Francisco, 1980).
[41] J. Voit, L. Perfetti, F. Zwick, H. Berger, G. Margaritondo, G. Grüner, H. Höchst, and M. Grioni, Science **290**, 501 (2000).